Brazilian Journal
of Chemical
Engineering

ISSN 0104-6632
Printed in Brazil

Vol. 21, No. 01, pp. 23 - 33, January - March 2004

# THE INFLUENCE OF STRUCTURAL PARAMETERS ON THE PERMEABILITY OF CERAMIC FOAMS

E. A. Moreira and J. R. Coury*

Departamento de Engenharia Química, Universidade Federal de São Carlos,
Phone +(55) (16) 260-8264, Fax +(55) (16) 260-8266,
Rod. Washington Luiz km 235, CEP 13565-905, São Carlos - SP, Brazil.
E-mail: jcoury@power.ufscar.br

*(Received: April 15, 2003 ; Accepted: July 3, 2003)*

**Abstract -** Ceramic foams are a new structural material, characterized by a high porosity and a large surface area and made of megapores interconnected by filaments. This results in a structure with low resistance to fluid flow, making them appropriate for use as a filter. This work studies the influence of several structural parameters, such as porosity, tortuosity, surface area and pore diameter, in predicting the permeability of ceramic foams. Foams with different pore densities were used as porous media. Permeability was measured utilizing water as the flowing fluid. The results show that the predicted permeability scatters widely with the parameters under study. Pore diameter was the structural parameter that best represented the media. An Ergun-type correlation was fitted to the data and represented very well the permeability of the media in all foams under the experimental conditions studied.
*Keywords*: Ceramic foams, permeability, flow through porous media.

## INTRODUCTION

Ceramics generally have good mechanical, chemical and thermal resistance (Dickenson, 1997). Because of their porosity, they are widely used as filters for hot gas cleaning (Lehtovaara, 1993; Eggerstedt et al., 1993), in the purification of liquid metals (Acosta et al., 1995) and as acoustic absorbers, bioreactors (Sheppard, 1993), heat exchangers, etc.

One type of ceramic media, cellular ceramics, have become an interesting alternative as structural components in the solid-fluid separation technology in the last several decades (Schwartzwalder and Sommers, 1963, Innocentini, 1997). Cellular ceramics consist of several open cells arranged in honeycomb or foam-like structures. These structures have a large number of interconnected pores, which produces low resistance to the flow of fluids. They also have low density and controlled pore size, and in an appropriate combination of ceramic materials and processing techniques, also show a very good performance in all applications of ceramic materials.

In general, the mechanical behavior and the structural characterization of ceramic foams are relatively well explored in the literature, but the same cannot be said for permeability, one of the main filtration parameters.

Most of the models used to determine permeability in these media are derived from correlations originally developed for granular beds, and this often produces gross deviations. Due to the unique characteristics of the foams, one of the main difficulties in developing these models is in identifying structural characteristics that represent the cell media realistically.

This work examines the effect of a number of structural parameters, such as effective porosity (i.e., the porosity that effectively contributes to the fluid flow), tortuosity, specific surface area and pore

*To whom correspondence should be addressed

diameter, in the prediction of bed permeability based on models found in the literature. One of the models was applied as derived for granular beds and the others had already been adapted to cell media.

Effective porosity was obtained by the stimulus-response method (time of residence) and pore diameter and surface area were obtained by image analysis. The latter was also obtained by the use of correlations proposed by Richardson et al. (2000) and Gibson and Ashby (1988). Tortuosity was obtained by measuring the electric resistivity of the medium. The ceramic foams utilized were made of SiC-$Al_2O_3$, and have linear pore densities of 8, 20 and 45 pores per inch (ppi). Permeability was measured utilizing water at ambient temperature as the flowing fluid.

## PERMEABILITY OF POROUS MEDIA

The permeability of a fluid while flowing through a porous medium is usually quantified by the Forchheimer equation, described as

$$\frac{\Delta P}{L} = \frac{\mu}{k_1} v + \frac{\rho}{k_2} v^2 \tag{1}$$

where $\Delta P$ is the pressure drop, L is thickness of the medium, $\rho$ and $\mu$ are the viscosity and the density of the fluid, respectively, and v is the volumetric flow rate per unit of cross-sectional area of the flowing fluid.

Parameters $k_1$ and $k_2$ are usually referred to as the Darcyan and non-Darcyan permeability parameters, respectively. These parameters are assumed to incorporate the structural properties of the medium and to be a function of bed characteristics only.

Of the correlations that incorporate characteristics of the porous medium, the one proposed by Ergun (1952) is the most frequently used and it was derived from the flow through granular beds. This correlation has the same general form as that of Equation (1) and is expressed as

$$\frac{\Delta P}{L} = 150\frac{(1-\varepsilon)^2}{\varepsilon^3}\frac{\mu v}{d_p^2} + 1.75\frac{(1-\varepsilon)}{\varepsilon^3}\frac{\rho v^2}{d_p} \tag{2}$$

where $\varepsilon$ is the bed porosity and $d_p$ is the median surface-volume diameter of the particles that form the granular bed.

Basing their research on the same idea and working with several forms of spherical and nonspherical particles, a number of researchers have proposed different values for the numerical constants in Equation (2), but no relevant improvement has been achieved. A thorough review of this subject is presented by Macdonald et al. (1979).

For cell media, there are few proposed correlations and these are not very general. Of these correlations that of DuPlessis et al. (1994) is worth mentioning. It assumes that the cell medium is formed of cubic unit cells, resulting in the following correlation:

$$\frac{\Delta P}{L} = \frac{36\tau(\tau-1)}{\varepsilon^2}\frac{\mu v}{d_{pore}^2} + \frac{2.05\tau(\tau-1)}{\varepsilon^2(3-\tau)}\frac{\rho v^2}{d_{pore}} \tag{3}$$

where $\tau$ is the medium tortuosity and $d_{pore}$ is the pore diameter.

A more recent correlation, proposed by Richardson et al. (2000) and based on the work of Gibson and Ashby (1988), assumes that the cellular medium is formed of cells of the type shown in Figure 1. For these authors, the expression for $\Delta P/L$ in S.I. units is given by

$$\frac{\Delta P}{L} = \frac{\alpha a_{vs}^2(1-\varepsilon)^2}{\varepsilon^3}\mu v + \frac{\beta a_{vs}(1-\varepsilon)}{\varepsilon^3}\rho v^2 \tag{4}$$

where parameters $\alpha$ and $\beta$ are given by

$$\alpha = 973 d_{pore}^{\,0.743}(1-\varepsilon)^{-0.0982} \tag{5}$$

$$\beta = 368 d_{pore}^{\,-0.7523}(1-\varepsilon)^{0.07158} \tag{6}$$

According to the authors, the specific surface area can be calculated by

$$a_{vs} = \frac{12.979[1-0.971(1-\varepsilon)^{0.5}]}{d_{pore}(1-\varepsilon)^{0.5}} \tag{7}$$

While for granular media the dependence of particle diameter was correctly quantified by Ergun, the role of pore diameter in a cellular structure is not clear. Another aspect to be considered is how total porosity and effective porosity (i.e., the porosity that contributes to the flow of the fluid inside the porous medium) influence the permeability parameters. These parameters as well as bed tortuosity and specific surface area were measured and used in the respective correlations.

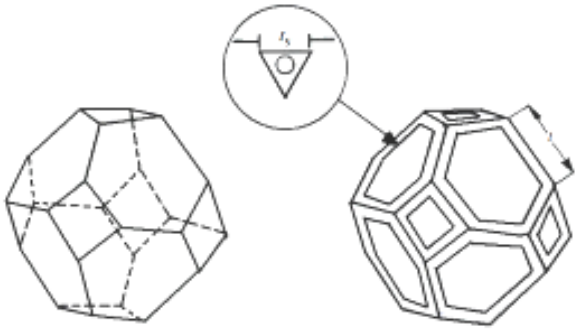

**Figure 1:** Diagram of the cell conceived by Richardson et al.(2000).

## MATERIALS AND METHODS

### The Cell Media

The ceramic foams utilized in this work were manufactured by the replica technique, whereby the filaments of an organic foam are coated with a ceramic suspension. A subsequent thermal treatment removes the organic material, leaving the ceramic material in the substratum. This method allows production of regular structures since good quality organic foams are used as matrixes. The foams are specified commercially by the number of pores per linear inch (ppi) and attention must be paid to their uniformity.

The ceramic foams were made from SiC-$Al_2O_3$ powders, and the polymeric foams used as matrixes were polyurethane foams with highly uniform pores. The foams were soaked with the ceramic mix, followed by calcination. Details are given in Moreira et al (1999). Also, a fixed bed of glass spheres with diameter of 2.95 mm was used for comparison. All media were made in the DEQ and DEMa laboratories at the Universidade Federal de São Carlos. Figure 2 illustrates the foams utilized, which had pore densities of 8, 20 and 45 pores per inch (ppi).

### Permeability Measurements

A general view of the equipment used for measurement of permeability of the ceramic foams is illustrated in Figure 3. The fluid used in the experiments was water at ambient temperature. For the water permeability measurements, the mass flow rate was obtained by weighing water that flowed through the sample in a given period of time. Pressure drop was measured with a micromanometer (Furness FC016). The experiments were carried out in triplicate and pressure drop was plotted as a function of fluid superficial velocity, v.

(a) (b) (c)

**Figure 2:** Ceramic foams with (a) 8 ppi, (b) 20ppi and (c) 45ppi.

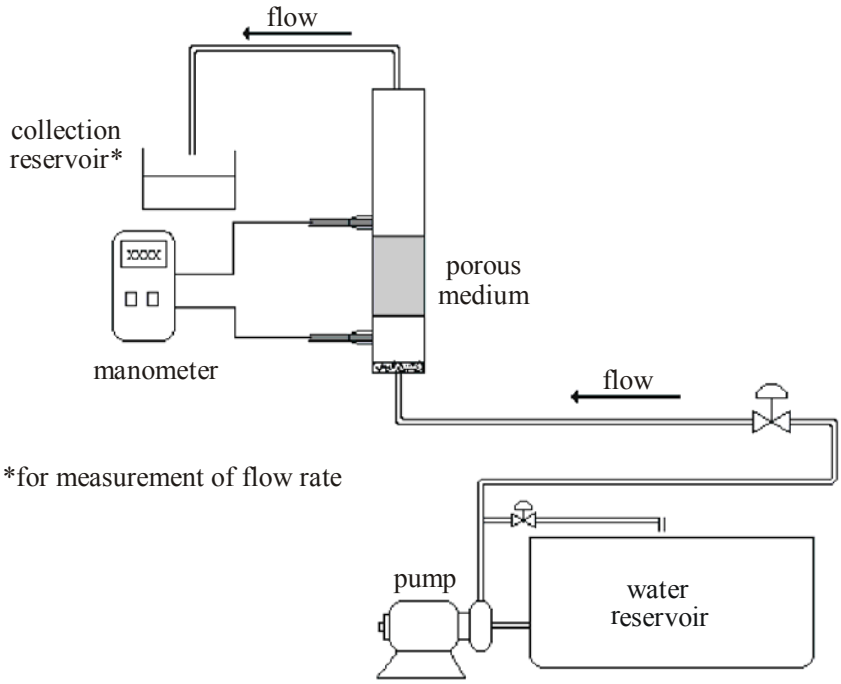


**Figure 3:** General view of the equipments for the permeability measurements.

**Total and Effective Porosity**

The total porosity of a porous bed is defined as

$$\varepsilon = \frac{\text{volume of the open voids}}{\text{total bed volume}} = \frac{V_F}{V_T} \tag{8}$$

But not all the fluid that fills the voids within a porous medium flows when a pressure difference is applied. Part of this fluid remains stagnant and does not contribute to the fluid flow rate. Effective porosity, i.e. that porosity which contributes for the flow, can be defined as

$$\varepsilon^* = \frac{\text{vol. occupied by the flowing fluid}}{\text{total bed volume}} = \frac{V_F^*}{V_T} \tag{9}$$

If a porous bed is fed with a fluid with a volumetric flow rate Q, then

$$Q = \frac{\text{volume of flowing fluid}}{\text{time}} = \frac{V_F^*}{t^*} \tag{10}$$

where t* is the time of flow of the fluid through the medium.

For the bed without the porous medium, with the same total volume, the flow rate is given by

$$Q = \frac{\text{total volume}}{\text{time}} = \frac{V_T}{t} \tag{11}$$

For the same flow rate, effective porosity (Equation 9) can be calculated by equating Equations (10) and (11). The result is

$$\varepsilon^* = \frac{t^*}{t} \tag{12}$$

Therefore ε*, effective porosity, can be obtained from the ratio of the residence times in a given volume, with and without porous medium, respectively, for the same flow rate Q.

The total porosity of the media can be measured utilizing Equation 13:

$$\varepsilon = 1 - \frac{\rho_b}{\rho_s} \tag{13}$$

where $\rho_b$ is the apparent density of the sample (mass/total sample volume) and $\rho_s$ is the solid phase density, measured here with a Micromeritics Helium Picnometer.

**The Residence Time Estimate**

Average residence time can be obtained from the residence time distribution (RTD), using the stimulus-response technique. In this technique, a nonreactive tracer pulse is injected into the flowing fluid as it enters the porous bed and the concentration of this tracer is measured at the exit as a function of time.

In this case, Levenspiel (2000) defined the average residence time as

$$\bar{t} = \frac{\int_0^\infty tCdt}{\int_0^\infty Cdt} = \frac{\sum t_i C_i \Delta t_i}{\sum C_i \Delta t_i} \quad (14)$$

in which $\bar{t}$ (assumed here to be t*) is the average residence time and $C_i$ is the concentration of the tracer at the exit of the porous bed at time $t_i$.

For determination of residence time, a system of data acquisition, which consisted of a duct containing the porous medium, was developed. A pulse of a previously calibrated NaCl solution was injected before the medium, and a probe (CBL 2) was placed after it. The probe was connected to a TI-89 calculator that measured and stored the concentration of the tracer as a function of time. Figure 4 illustrates the rig utilized for the residence time measurements.

**Tortuosity**

Sheidegger (1974) defined tortuosity as the ratio of the real length that the fluid travels inside a medium ($L_e$) to the thickness of the medium (L). The author suggests that it can be obtained by measuring the formation factor, F, which is given by the electrical resistivity of the porous medium completely saturated with a conductive solution ($\delta_m$) divided by resistivity of the solution alone ($\delta_s$). Therefore

$$F = \frac{\delta_m}{\delta_s} \quad (15)$$

and tortuosity is given by

$$\tau = \varepsilon F \quad (16)$$

The tortuosity tests were conducted in the equipment shown in Figure 5. For these experiments, Ag/AgCl reference electrodes were used in a Luggin capillary filled with a 0.3 mol KCl solution. These electrodes were connected to a test chamber and to a voltmeter to measure the potential difference. In the test chamber, a 0.1 mol $H_2SO_4$ solution was used as thed test solution. The current was supplied by a source that varied from 0 to 15 mA. For the experiments, the highest current utilized was of 8mA, so that hydrogen formation could be avoided.

The experimental procedure consisted of measuring the potential difference for each value of applied current, for the test chamber filled with the solution of $H_2SO_4$ alone and also for the chamber filled with the porous medium and the solution. The potential differences measured were plotted as a function of current, giving straight lines, whose slopes are the resistivities of the solution and of the medium, respectively. Tortuosity was calculated utilizing Equation (16).

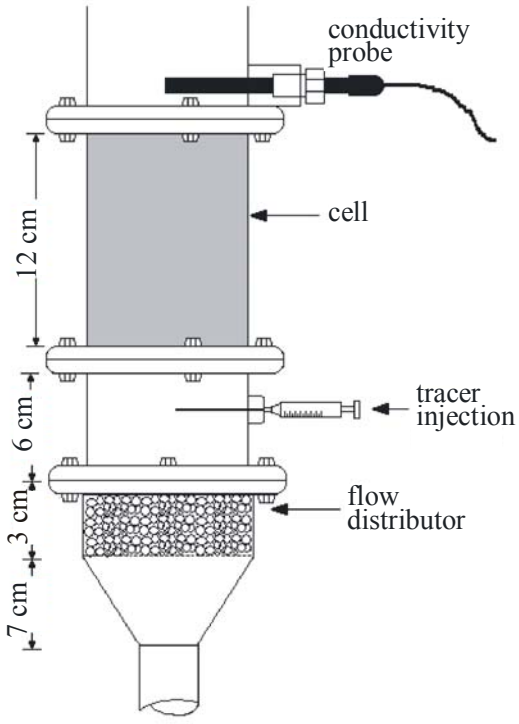


**Figure 4:** The rig utilized for the residence time measurements.

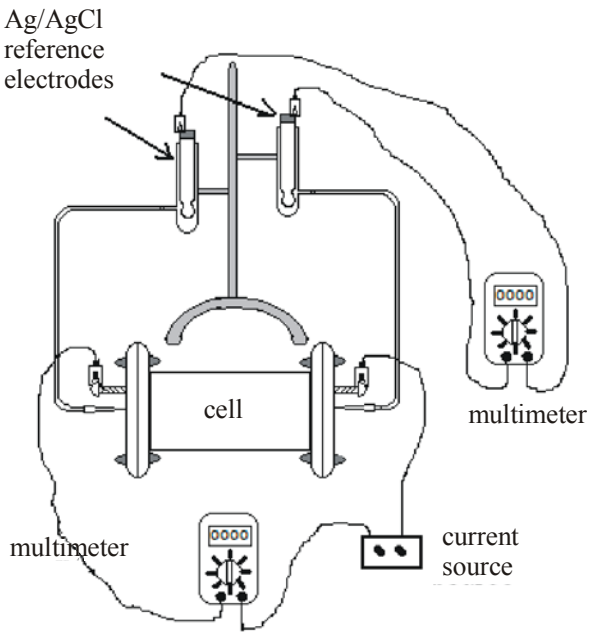


**Figure 5:** Diagram of the equipment for the tortuosity measurements.

### Pore Diameter and Specific Surface Area

The diameter of the pores for each sample was obtained by image analysis, using the Image Pro-Plus software. The specific surface area was obtained by measuring (by image analysis) the perimeter of the solid phase of a cross section of the foam and multiplying it by the length, $L_e$, of the tortuous path, obtained from the tortuosity measurements.

## RESULTS AND DISCUSSION

### Experimental Measurement of the Structural Parameters

Table 1 lists the structural parameters measured. Pore diameter decreased with the increase in linear pore density, ppi, as expected. Less obvious, total porosity of the bed decreased with the increase in ppi, probably due to pore clogging during foam formation, more likely to occur in smaller pores. This is confirmed by the tortuosity and the specific surface area results, as both increase with ppi: the more clogged the medium the more tortuous the fluid path and the higher the total wall surface. The tortuosity values are similar to reported values from the literature (Montillet et al., 1992). The specific surface areas measured are similar those predicted by Equation (7).

Table 1 also shows that the effective porosities of the foam are somewhat smaller than the total porosities, indicating that an appreciable amount of fluid remains stagnant (or recirculates) within the bed. As expected, these stagnant regions decrease as the flow rate increases. These smaller porosities are reflected accordingly in the effective tortuosities and specific surface area (the latter can be understood as the interface between the flowing and the stagnant fluid).

**Table 1: Measured pore diameters, porosities, tortuosities and specific surface areas**.

| | | Porosity | | Tortuosity | | Specific surface area | |
|---|---|---|---|---|---|---|---|
| **Foam** | **$d_{pore}$ (mm)** | **ε** | **ε*[a]** | **τ** | **τ*[b]** | **$a_{vs}$ ($m^2/m^3$)** | **$a^*_{vs}$[b] ($m^2/m^3$)** |
| 8ppi | 2.30 | 0.94 | 0.74/0.77 | 1.68 | 1.38 | $1.83 \times 10^4$ | $0.63 \times 10^4$ |
| 20ppi | 0.80 | 0.88 | 0.71/0.73 | 1.71 | 1.42 | $1.92 \times 10^4$ | $0.71 \times 10^4$ |
| 45ppi | 0.36 | 0.76 | 0.50/0.62 | 1.84 | 1.50 | $2.34 \times 10^4$ | $1.20 \times 10^4$ |
| gb[c] | 2.95 | 0.36 | 0.37/- | | | | |

[a]the two values reported refer to Q = 0.4 and 2.0 l/min, respectively.
[b]the symbol * refers to parameter calculated utilizing effective porosity ε∗ for q = 2 l/min.
[c]glass beads

**Permeability Measurements**

Figure 6 shows the permeability curves for the foams. These tests were carried out in triplicate and the average and deviations are shown, indicating the good reproducibility of the procedure. A wide range Reynolds number for the bed, Re, varying from $5\times10^2$ to $2.5\times10^4$, was covered.

**Comparison with Correlations from the Literature**

Figure 7 shows the permeability curve for a fixed bed of glass beads, utilizing the same equipment as for the foams. The results are very well represented by the classical Ergun equation, demonstrating the reliability of the apparatus.

Figure 8 shows a comparison of the results with the theoretical correlations from the literature. In these curves, all the structural parameters utilized (porosity, tortuosity, specific surface area) were based on the total porosity of the foams. Figs. 8a, 8b and 8c refer to flow through the foams with 8, 20 and 45 ppi, respectively. Four theoretical curves are plotted in all figures: (i) the Ergun (1952) correlation (Eq.2) replacing particle diameter, $d_p$, by pore diameter, $d_{pore}$, as suggested by Philipse and Schram (1991); (ii) the DuPlessis et al. (1994) correlation (Eq.3); (iii) the Richardson et al. (2000) correlation (Eq.4) with $a_{vs}$ calculated by Equation (7); and (iv) the Richardson et al. (2000) correlation (Eq.4) with the experimental $a_{vs}$ measured here.

The comparison reveals that all theoretical predictions increase with increasing ppi. The general shape of all prediction curves was similar to that of the experimental points, but they did not give accurate predictions of the pressure drop in the bed. The predictions vary from an underestimate of the pressure drop for 8ppi (all but Eq.3) to an overestimate for 45 ppi. Of the four correlations tested, the Richardson et al. (2000) equation (Eq.4) utilizing the experimental value of $a_{vs}$ was the one that had smaller deviations, as can be seen in Table 2 - deviations varied between 47 and 57%, which is fairly high.

Figure 9 shows results equivalent to those in Figure 8, but for the structural parameters (porosity, tortuosity, specific surface area) based on the effective porosity of the foams. The results reveal that the predictions based on the effective parameters tended to diminish the scatter between the theoretical curves, compared to the corresponding curves shown above. In these results the pressure drop was overestimated in all cases, but the tendency of the overestimate to increase with increasing ppi remains. Here again, the Richardson et al. (2000) equation (Eq.4) utilizing the experimental value of $a_{vs}$ was the one that had the smallest deviations, as can be seen in Table 2 - deviations varied between 56 and 109%, which is still very high and scattered.

In all, no correlation was able to predict pressure drop, in all the foams and under all the conditions studied, and large deviations (as high as 654%) can be observed in Table 2.

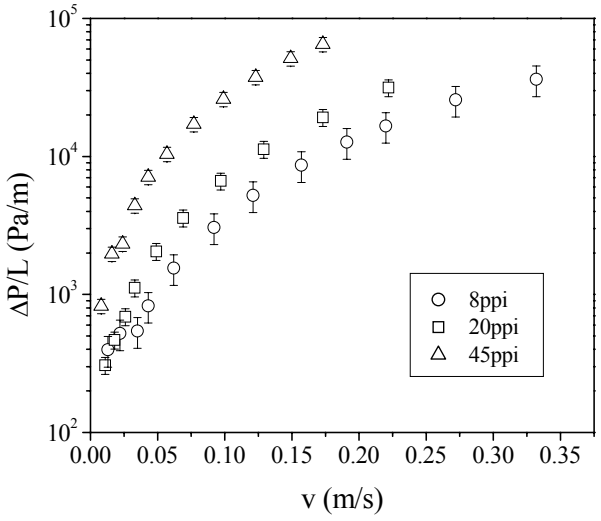


**Figure 6:** The permeability tests performed.

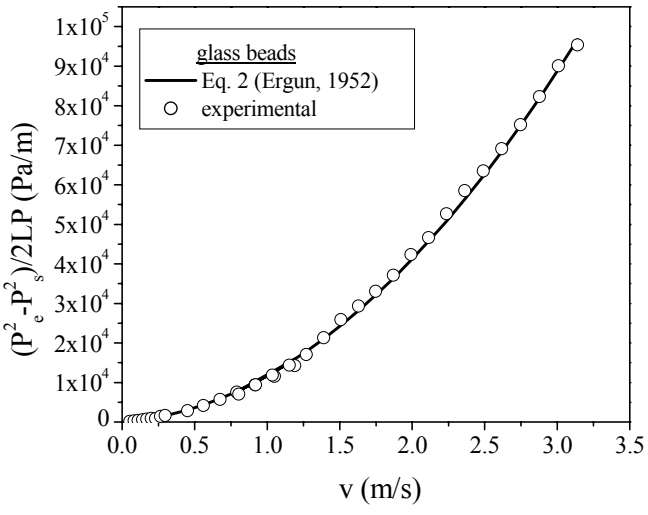


**Figure 7:** Comparison between the experimental data and the curve predicted by the Ergun correlation (Eq.2) for a fixed bed of glass beads.

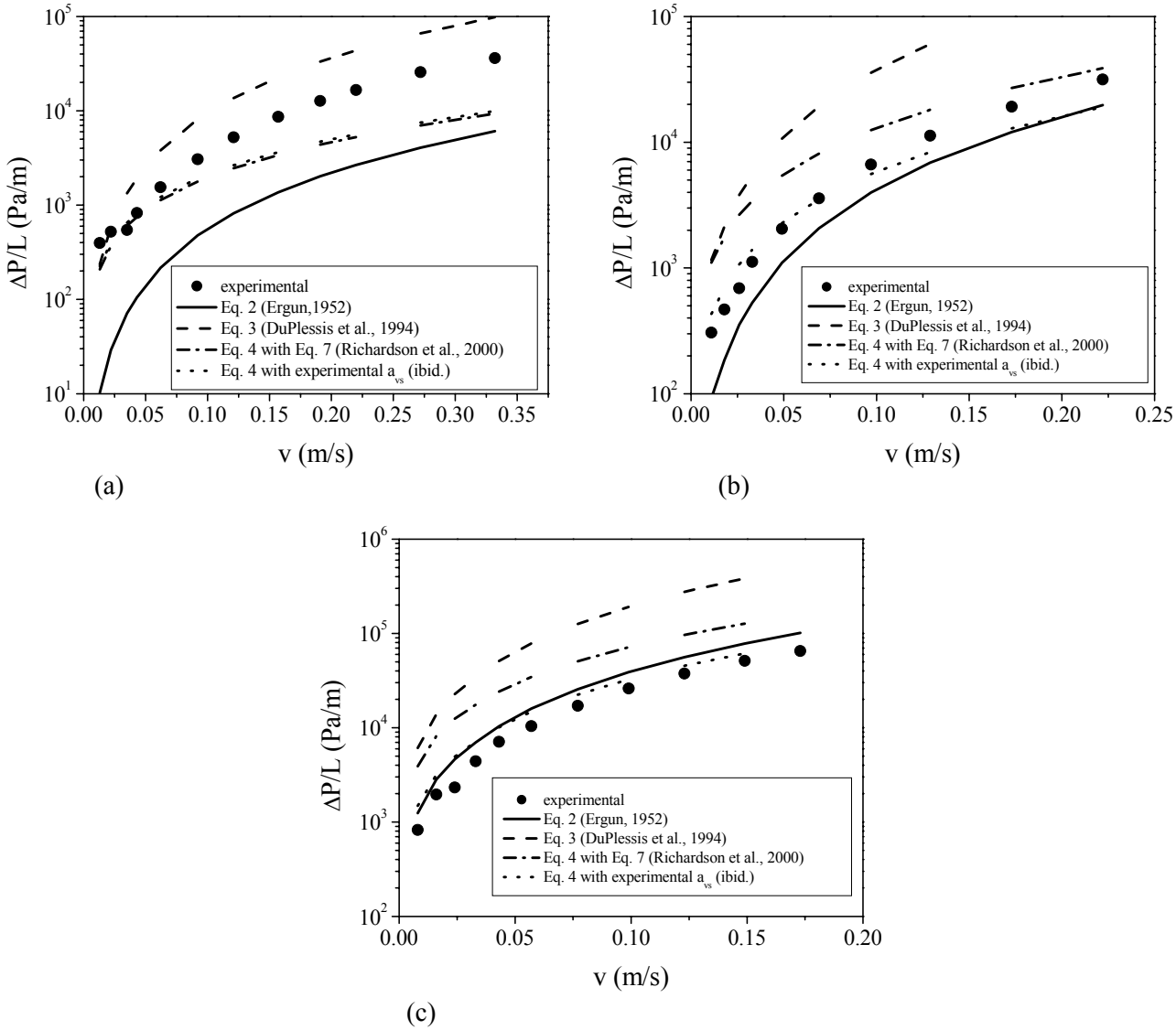


**Figure 8:** Comparison between the experimental data and the curves predicted by models from the literature, utilizing *total* porosity, tortuosity and specific surface area for (a) 8ppi, (b) 20ppi and (c) 45ppi.

**Table 2: Maximum deviations for the correlations tested.**

| | Maximum deviation δ (%)[a] | | | | | |
|---|---|---|---|---|---|---|
| | ε | | | ε* | | |
| **Correlation** | **8ppi** | **20ppi** | **45ppi** | **8ppi** | **20ppi** | **45ppi** |
| Ergun (1952) (Eq. 2) | 87 | 47 | 60 | 31 | 180 | 482 |
| DuPlessis et al. (1994) (Eq. 3) | 201 | 471 | 654 | 71 | 254 | 292 |
| Richardson et. al. (2000) (Eqs. 4 and 7) | 54 | 150 | 247 | 110 | 415 | 484 |
| Richardson et. al. (2000) (Eq.4 with exp. $a_{vs}$) | 57 | 50 | 47 | 109 | 56 | 90 |
| Proposed correlation (Eq. 17) | 8 | 5 | 7 | - | - | - |

[a] $\delta = \frac{1}{n}\sum_{1}^{n}\left|\frac{(y_{ex} - y_{cal})}{y_{ex}}\right| \times 100$ ; where $y_{ex}$ and $y_{cal}$ are the experimental and calculated values.

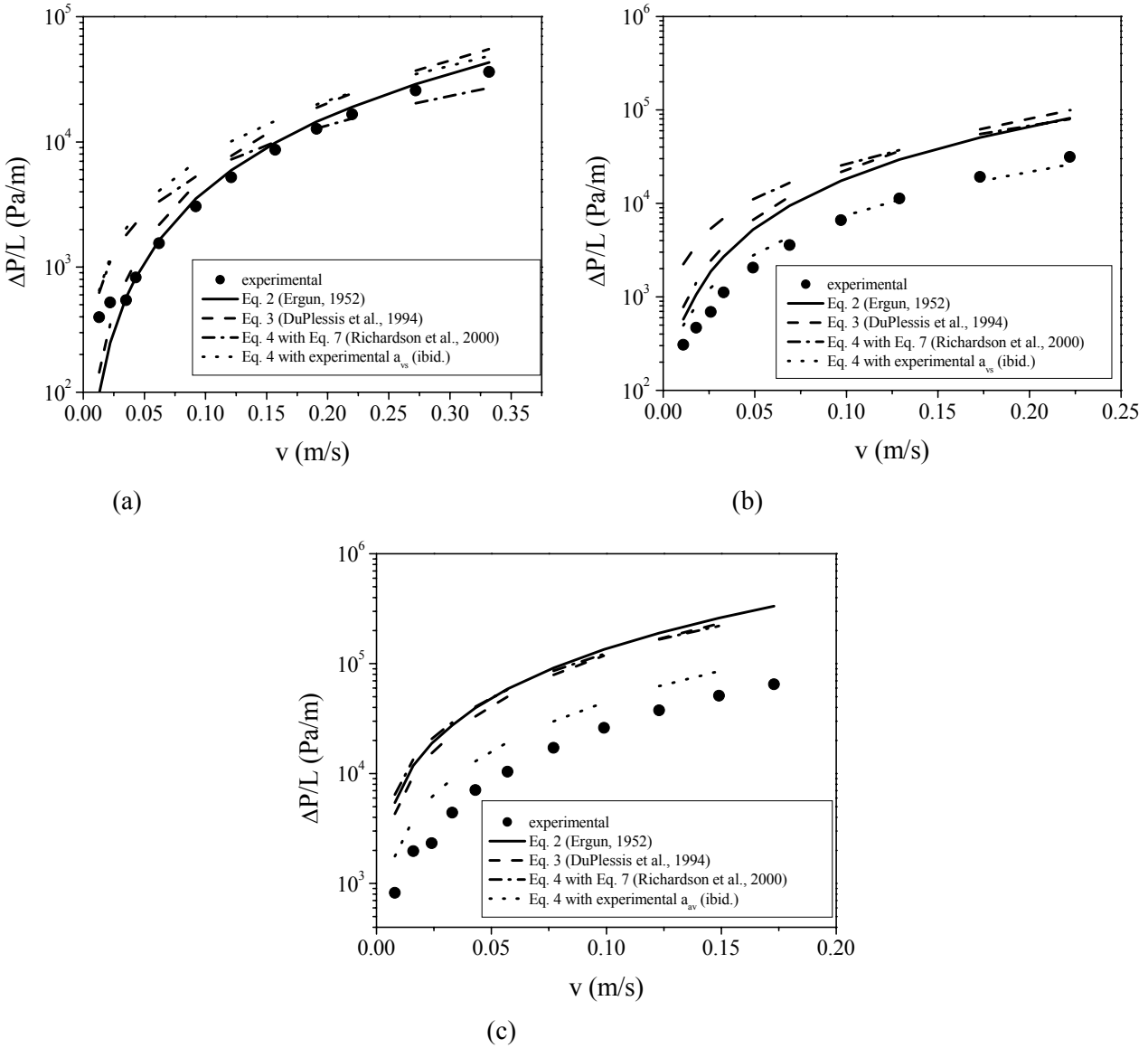


**Figure 9:** Comparison between the experimental data and the curves predicted by models from the literature, utilizing *effective* porosity, tortuosity and specific surface area for (a) 8ppi, (b) 20ppi and (c) 45ppi.

## The Proposed Correlation

As no single correlation covered the whole range studied, a multi-parameter fit of the experimental results was carried out. The Ergun equation was taken as the point of departure, and numerous combinations were tested. Structural parameter $d_p$ (as the foams have no particle diameter) was replaced by other structural parameters ($a_{vs}$, $\tau$). The two porosities ($\varepsilon$,$\varepsilon^*$) were used, and the numerical constants 150 and 1.75 replaced by another numerical values.

The best fit obtained was that utilizing pore diameter, $d_{pore}$, and the total porosity, $\varepsilon$, as structural parameters. The final correlation for SI units has the following form:

$$\frac{\Delta P}{L} = 1.275\times10^{9}\frac{(1-\varepsilon)^2}{\varepsilon^3}\frac{\mu v}{d_{pore}^{-0.05}} + \\ +1.89\times10^{4}\frac{(1-\varepsilon)}{\varepsilon^3}\frac{\rho v^2}{d_{pore}^{-0.25}} \qquad (17)$$

Figure 10 shows a comparison of the measured pressure drop with the one predicted by Equation (17). Very good agreement between measurement and prediction can be seen, with small deviations (below 8%) in all the foams and under the conditions studied, as listed in Table 2.

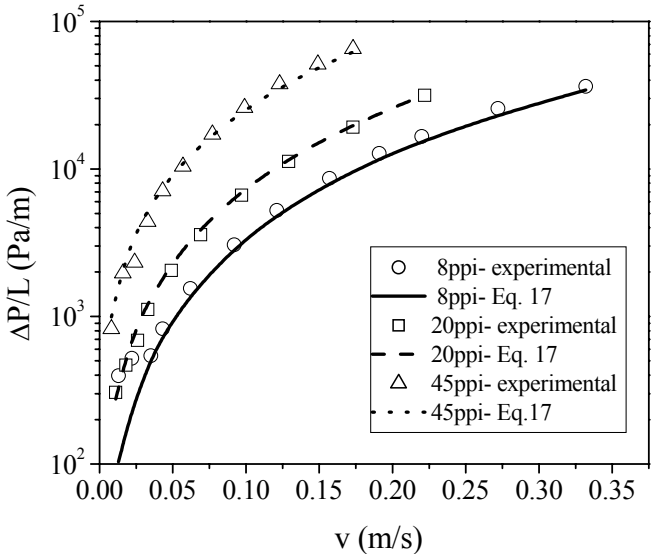


**Figure 10:** Comparison between the experimental data and the curves predicted by the proposed Equation (17).

## CONCLUSIONS

Ceramic foams, obtained from a SiC-$Al_2O_3$ mixture utilizing the replica technique, were tested as filtering medium. Their structure was quantified by measuring total and effective porosity, tortuosity and specific surface area. These structural parameters were then used to test the validity of several correlations for permeability prediction by comparing them with experimental data. No available correlation could predict the pressure drop in all the foams studied. An Ergun-type empirical correlation, obtained by data fitting, was proposed.

## ACKNOWLEDGEMENTS

The authors are indebted to FAPESP (proc. 98/15076-0) and to PRONEX-FINEP for the financial support that made this work possible. They are also indebted to Dr Vania Salvini, Dr Victor Pandolfelli and Dr Murilo Innocentini at DEMa/UFSCar for their invaluable help in the manufacture of the ceramic media and to Luis Ruotolo for the resistivity measurements.

## NOMECLATURE

| | | |
|---|---|---|
| $a_{vs}$ | specific surface area | $[L^{-1}]$ |
| $C_i$ | tracer concentration at the bed exit at time $t_i$ | $[ML^{-3}]$ |
| D | bed diameter | [L] |
| $d_p$ | particle diameter | [L] |
| $d_{pore}$ | pore diameter | [L] |
| F | formation factor | [-] |
| $k_1$ | Darcyan permeability coeff. | $[L^2]$ |
| $k_2$ | non-Darcyan permeab. coeff. | [L] |
| L | bed thickness | [L] |
| $L_e$ | real (tortuous) length traveled by the flowing fluid | [L] |
| Q | volumetric flow rate | $[L^3t^{-1}]$ |
| Re | Reynolds number of the bed ($\rho vD/\mu$) | [-] |
| t | time of flow through the volume without the porous medium | [t] |
| t* | time of flow through the volume with the porous medium | [t] |
| $\bar{t}$ | average residence time | [t] |
| v | volumetric flow rate per bed cross-sectional area | $[Lt^{-1}]$ |
| $V_F$ | volume of the open voids | $[L^3]$ |
| $V_F^*$ | volume occupied by the flowing fluid | $[L^3]$ |
| $V_T$ | total bed volume | $[L^3]$ |
| $\Delta P$ | pressure drop | $[ML^{-1}t^{-2}]$ |

### *Greek Letters*

| | |
|---|---|
| $\alpha$ | empirical parameter of Equation (7) |
| $\beta$ | empirical parameter of Equation (8) |

| | | |
|---|---|---|
| $\delta_c$ | electrical resistivity of the conductive solution | [H] |
| $\delta_m$ | electrical resistivity of the medium saturated with the solution | [H] |
| $\varepsilon$ | total porosity of the bed | [-] |
| $\varepsilon^*$ | effective porosity of the bed | [-] |
| $\rho$ | fluid density | $[ML^{-3}]$ |
| $\rho_b$ | apparent density of the bed | $[ML^{-3}]$ |
| $\rho_s$ | solid density | $[ML^{-3}]$ |
| $\mu$ | fluid viscosity | $[ML^{-1}t^{-1}]$ |
| $\tau$ | tortuosity | [-] |

## REFERENCES


Acosta, F.A., Castillejos, A.H., Almanza, J.M. and Flores, A., An Analysis of Liquid Flow through Ceramic Porous Media Used for Molten Metal Filtration. Metallurgical and Materials Processing Transactions B, vol. 26B, p. 159 (1995).

Dickenson, C., Filters and Filtration Handbook. 3rd ed., Elsevier Science Publishers, Oxford (1997).

DuPlessis, P., Montillet, A., Comiti, J. and Legrand, J., Pressure Drop Prediction for Flow through High Porosity Metallic Foams, Chemical Engineering Science, 49[21], p. 3545 (1994).

Eggersted, P.M., Zievers, J.F. and Zievers, E.C., Choose the Right Ceramic for Filtering Hot Gases. Chemical Engineering Progress, January, p. 62 (1993).

Ergun, S., Flow through Packed Columns, Chemical Engineering Progress, 48 [2], p. 89 (1952).

Gibson, L.J. and Ashby, M.F., Cellular Solids - Structure & Properties, Pergamon Press, Cambridge (1988).

Innocentini, M.D.M. Ph.D. diss., Universidade Federal de São Carlos (1997).

Lehtovaara, A. and Mojtahedi, W., Ceramic Filters Behavior in Gasification. Bioresource Technology, 46, p. 113 (1993).

Levenspiel, O., Engenharia das Reações Químicas, 3rd ed., Edgard Blucher Ltda, São Paulo (2000).

Macdonald, I.F., El-Sayed, M.S. and Dullien, F.A., Flow through Porous Media - the Ergun Equation Revisited, Industrial and Engineering Chemistry Fundamentals, 18[3], p. 199 (1979).

Montillet, A., Comiti, J. and Legrand, J., Determination of Structural Parameters of Metallic Foams from Permeametry Measurements, Journal of Materials Science, vol. 27, pp. 4460-4464 (1992).

Moreira, E.A., Innocentini, M.D.M., Salvini, V.R., Pandolfelli, V.C. and Coury, J.R., Permeability of Ceramic Foams IN: Proceedings of the XXVII ENEMP - Brazilian Congress on Particulate Systems, p. 241 (1999).

Philipse, A.P. and Schram, H.L., Non-Darcian Airflow through Ceramic Foams, Journal of the American Ceramic Society, 74[4], pp. 728-732 (1991).

Richardson. J.T., Peng, Y. and Remue, D., Properties of Ceramic Foam Catalyst Supports: Pressure Drop, Applied Catalysis A: General, vol. 204, p. 19 (2000).

Schwarzwalder, K. and Sommers, A.V., Method of Making Porous Ceramic Articles, U.S. Patent 3.090.094 (1963).

Sheidegger, A.E., The Physics of Flow through Porous Media, 3rd ed., Univ. Toronto Press, Toronto (1974).

Sheppard, L.M., Porous Ceramics: Processing and Applications, In: Ceramic Transactions - Porous Materials, The American Ceramic Society Bulletin, vol.31, p. 3 (1993).